Arch. Mech., 37, 6, pp. 643–659, Warszawa 1985

The Bauschinger effect in cyclic plasticity

TH. LEHMANN (BOCHUM), B. RANIECKI and W. TRĄMPCZYŃSKI (WARSZAWA)

THE SIMPLE plastic shear and simple plastic tension tests of 21CrMoV57 steel are performed The specimens are loaded monotonically and cyclically under controlled amplitude of plastic strains at room temperature. Using the technique of successive unloading, the standard physical quantities and the stress jump corresponding to opposite directions of plastic straining are measured. The jump represents, in a certain sense, the Bauschinger effect. For ellipsoidal yield surfaces the results obtained enable a direct verification of kinematic hardening laws.

Przeprowadzono próby plastycznego prostego ścinania i prostego rozciągania stali 21CrMoV57. Próbki poddano obciążeniom monotonicznym i cyklicznie zmiennym przy danej i kontrolowanej amplitudzie odkształceń plastycznych, w temperaturze pokojowej. Obok standardowych wielkości fizycznych prześledzono zmiany w czasie nowej wielkości — różnicy pomiędzy rzeczywistym naprężeniem w podstawowym programie i naprężeniem uplastyczniającym materiał przy przeciwnym kierunku obciążania. Taka wielkość reprezentuje efekt Bauschingera. Cel ten osiągnięto stosując technikę kolejnych odciążeń. Wyniki umożliwiają bezpośrednią weryfikację niektórych równań ewolucji dla parametrów wzmocnienia.

Проведены испытания пластического простого сдвига и простого растяжения стали 21 CrMoV 57. Образцы подвергнуты монотоническим и циклически переменным нагружениям, при заданной и контролируемой амплитуде пластических деформаций, в комнатной температуре. Кроме стандартных физических величин прослежены изменения во времени новой величины — разницы между действительным напряжением в основной программе и напряжением переводящим материал в пластическое состояние, при обратном направлении нагружения. Такая величина представляет эффект Баушингера. Эта цель достигнута, применяя технику последовательных нагружений. Результаты дают возможность непосредственно проверить некоторые уравнения эволюции для параметров упрочнения.

1. Introduction

THE BEHAVIOUR of plastically strained solids under monotonic and cyclic loading is very complex, even when all the rate effects are neglected. Therefore, new concepts to include into the theoretical frame some observed strain history effects [1–4] are recently introduced. One of such concepts is based upon the assumption that, apart from the traditional yield surface in the stress space, there exists one or more surfaces in a space of the tensors describing the motion of the centre of the yield surface. This tensor is sometimes identified with a phenomenological measure of microstresses. The evolution law for microstresses and the law of evolution for the isotropic part of hardening are usually postulated first, and then they are jointly verified by means of the data obtained from the measurements of global strain–stress curves.

Since such data are insufficient for unique separation of kinematic and isotropic hardening, the investigation of new concepts requires measurements of some additional physical quantity. The objective of this work is an experimental determination of such

a quantity; it is defined as the difference between the stress tensor associated with the actual plastic strain-rate vector in the basic program, and the stress tensor which would correspond to plastic strain rate vector which has an opposite direction. This difference represents, in a certain sense, the Bauschinger effect. It is believed that the obtained results will be useful for the verification of existing theories and that they will stimulate new ideas.

2. Motivation of the experiment

i) Denote by **S** the deviatoric part of stress tensor $\boldsymbol{\sigma}$, $S_{ij} = \sigma_{ij} - \delta_{ij}\sigma_{kk}/3$. Most of the theoretical models in cyclic plasticity (cf. e.g. [1–4]) employ the notion of a yield function f, which can be written in the following form

$$f(S_{ij} - \alpha_{ij}, H) = 0, \quad f(0, H) \leqslant 0, \tag{2.1}$$

where $\boldsymbol{\alpha}$ ($\alpha_{kk} = 0$) is sometimes identified with a macroscopic measure of microstresses. The letter H denotes symbolically the set of other possible parameters which describe the history of plastic strains.

The experimental investigations concerning the possible shape of yield surfaces and its properties under simple loading programs and under cyclic loading have been performed in a number of papers [5–7] (the review may be found in [8]). In the latter case the position and the shape of the yield surface were determined only at some chosen instants of a cyclic loading program. The obtained results are still insufficient for satisfactory verification of the law of kinematic hardening.

The basic theoretical problem is not only the description of the shape of the yield function but also the description of the motion of this surface through appriopriate choice of hardening parameters and the deduction of the evolution laws for the parameters. The basic difficulty consists in the fact that the hardening parameters, in particular the parameter $\boldsymbol{\alpha}$, have no universal operational definition. Each attempt to give an experimental definition of the parameter $\boldsymbol{\alpha}$ must be connected with a definite approximation of the description of all the yield surfaces generated by a given program of cyclic loadings. The complexity of phenomena observed under cyclic loadings constitutes an additional difficulty in searching the adequate evolution laws. It is not surprising, therefore, that in many theoretical treatments one frequently adopts rather drastic approximation through the assumption that all yield surfaces possess the centres of symmetry. The Huber–Mises spheres are particular examples of such surfaces. The tensor $\boldsymbol{\alpha}$ may then be identified with the radius-vector of the centre of symmetry, and the basic aim of the theoretical models is a possibly accurate description of the motion of the yield surface in S-space.

Suppose that, in some experimental program, the deviator of plastic strain e^p_{ij} ($e^p_{ii} = 0$) is controlled. The derivation of an adequate law of evolution for $\boldsymbol{\alpha}$ could be simplified if during an experimental program, apart from the actual stresses **S** and strains some other quantities would be measured. The example of such quantity is discussed below.

ii) The equation of the family of yield surfaces (2.1) can be presented in the equivalent parametric form

$$S_{ij} - \alpha_{ij} = n_{ij} R(\mathbf{n}, H), \tag{2.2}$$

where n_{ij} is the unit "vector" of directions in S_{ij}-space

$$n_{ij}n_{ij} = 1, \quad n_{ii} = 0. \tag{2.3}$$

Four independent components of n_{ij} constitute the set of parameters of the equation (2.2) of a 4-dimensional yield surface in S-space. For regular yield conditions R is a differentiable function of n_{ij} and H. Without losing generality it can be assumed that f occurring in (2.1) is so chosen that

$$\frac{\partial f}{\partial S_{ij}} \frac{\partial f}{\partial S_{ij}} = 1 \quad (f = 0).$$

The associated plastic flow law can then be written in the form

$$\frac{\dot{e}^p_{ij}}{(\dot{e}^p_{mn}\dot{e}^p_{mn})^{1/2}} = \frac{\partial f}{\partial S_{ij}}. \tag{2.4}$$

Consider the process of proportional plastic straining

$$e^p_{ij} = m_{ij}e^p(t), \quad m_{ij}m_{ij} = 1, \quad m_{kk} = 0, \quad m_{ij} = \text{const}, \tag{2.5}$$

such that $e^p(0) = 0$, $\dot{e}^p(0) > 0$, and assume that initially ($t = 0$) the specimens are in annealed state

$$H = 0, \quad \alpha_{ij} = 0 \quad \text{for} \quad t = 0.$$

Substituting (2.5) and (2.2) into (2.4) one obtains the formal relationship between m_{ij} and n_{ij}

$$m_{ij}(\operatorname{sgn}\dot{e}^p) = F_{ij}(\mathbf{n}, H), \quad F_{ij} = \left.\frac{\partial f}{\partial S_{ij}}\right|_{\mathbf{S}-\boldsymbol{\alpha}=\mathbf{n}R} \tag{2.6}$$

from which it follows that m_{ij} is a unique function of $\mathbf{n}$ for every H provided that $\dot{e}^p$ does not change the sign. In the case of analytical yield function it can be assumed that $\mathbf{n}$ is also a unique function of $\mathbf{m}$.

Neglecting the time intervals during which the response of a material is purely elastic, one can use the length λ of plastic strain trajectory as an independent variable instead of the real time,

$$\lambda = \int_0^t |\dot{e}^p| \, dt_1. \tag{2.7}$$

From the equation (2.6) it follows that in those points of the trajectory where $\dot{e}^p$ changes its sign, not only $\mathbf{S}'$ but also $\mathbf{n}$ undergoes jumps. However, $\boldsymbol{\alpha}$ and H have to be continuous functions of λ since they represent a history of plastic straining and they do not change in the elastic domains. This observation motivates the application of techniques of "succesive unloadings" for the measurement of S_{ij}-jumps in the course of plastic straining. Knowledge of the evolution of $\mathbf{S}'$-jump contains additional information that enables a more direct verification of any evolution law for α.

The basic program $0-C$ of plastic straining is shown in Fig. 1a. The program is interrupted at point A where the specimen is unloaded and reloaded into reverse direction until the conventional small value η, say $\eta = 0.5 \cdot 10^{-3}$, of the increment of e^p is achieved. In such a way one can in an experimental program identify the stress vector S^R_{ij} (Fig. 1b).

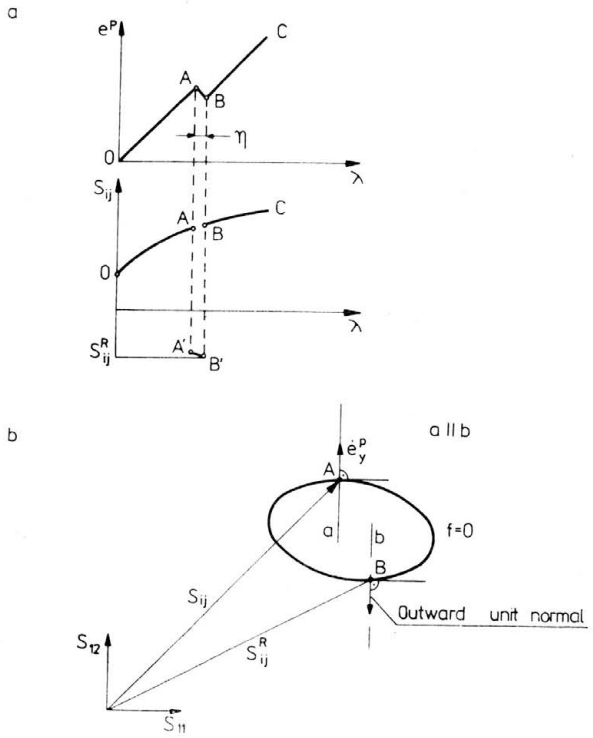

FIG. 1. Theoretical basis of unloading technique for hardening parameters determination.

Its one end lies at the yield surface at point B' where the plastic strain-rate vector has the direction opposite to that prescribed in the basic program. The interpretation of $\mathbf{S}-\mathbf{S}^R$ and $\mathbf{S}+\mathbf{S}^R$ follows from (2.2) and from the fact that $\boldsymbol{\alpha}$ is continuous at point A

$$
\begin{aligned}
2\mathbf{Y} &= \mathbf{S}-\mathbf{S}^R = \mathbf{n}R(\mathbf{n}, H)-\mathbf{n}^R R(\mathbf{n}^R, H),\\
2\boldsymbol{\Pi} &\equiv \mathbf{S}+\mathbf{S}^R = 2\boldsymbol{\alpha}+\mathbf{n}R(\mathbf{n}, H)+\mathbf{n}^R R(\mathbf{n}^R, H).
\end{aligned}
\tag{2.8}
$$

Two from the five tensorial quantities occuring in (2.8) ($\mathbf{Y}$ and $\boldsymbol{\Pi}$) can be measured. Two equations (2.8) are not sufficient for a unique determination of the remaining three quantities. Nevertheless, the experimental determination of $\mathbf{Y}$ and $\boldsymbol{\Pi}$ considerably enriches the possibility of verification of any theoretical idea.

iii) Consider the simple example. If actual yield surfaces are approximated by quadratic surfaces possessing the centre of symmetry (ellipsoides), then F_{ij} occuring in (2.6) and R occuring in (2.2) are odd and even functions of $\mathbf{n}$, respectively

$$
\mathbf{F}(-\mathbf{n}, H) = -\mathbf{F}(\mathbf{n}, H), \qquad R(-\mathbf{n}, H) = R(\mathbf{n}, H).
\tag{2.9}
$$

From $(2.9)_1$ it follows that $\mathbf{n}^R = -\mathbf{n}$. Hence

$$
\begin{aligned}
\mathbf{Y} &= (\mathbf{S}-\mathbf{S}^R)/2 = \mathbf{n}R(\mathbf{n}, H),\\
\boldsymbol{\Pi} &= (\mathbf{S}+\mathbf{S}^R)/2 = \boldsymbol{\alpha},
\end{aligned}
\tag{2.10}
$$

on account of (2.8) and $(2.9)_2$. Thus, for prescribed $e^p(t)$ the measurement of $\mathbf{Y}$ and $\boldsymbol{\Pi}$ gives full information concerning the changes in $\boldsymbol{\alpha}$, $\mathbf{n}$ and R, irrespectively of the specific

form of the quadratic function which describes the yield surfaces. In particular, if the successive yield surfaces are approximated by Huber–Mises spheres, then the length of radius R is independent of $\mathbf{n}$, $R = R(H)$ and $\mathbf{n} = \mathbf{m}$ (sgn $\dot{e}^p$).

iv) Let us define the projections of $\mathbf{Y}$ and $\mathbf{\Pi}$ onto $\mathbf{m}$ as follows:

$$\begin{aligned} Y &= |Y_{ij}m_{ij}| = |(S_{ij}-S^R_{ij})m_{ij}|/2 \geqslant 0, \\ \pi &= \Pi_{ij}m_{ij} = (S_{ij}+S^R_{ij})m_{ij}/2, \end{aligned} \tag{2.11}$$

so that

$$S_{ij}m_{ij} = \begin{cases} \pi+Y & \text{where} \quad (S_{ij}-S^R_{ij})m_{ij} > 0, \\ \pi-Y & \text{where} \quad (S_{ij}-S^R_{ij})m_{ij} < 0. \end{cases} \tag{2.12}$$

In the case of quadric surfaces the interpretation of Y and π follows from (2.10),

$$Y = |m_{ij}n_{ij}|R, \qquad \pi = \alpha_{ij}m_{ij}.$$

Thus π is the projection of $\boldsymbol{\alpha}$ on the direction m_{ij}, whereas Y equals the principal radius of an ellipsoide whenever $|m_{ij}n_{ij}| = 1$.

The objective of this paper is the experimental determination of Y and π, during cyclic and monotonic loading of a specimen under controlled plastic strain. The experiments concern two simplest cases:

a) simple plastic shear,

b) simple plastic tension (compression).

In the case (a) the only non-zero components of m_{ij} and e^p_{ij} are

$$\begin{aligned} m_{12} &= m_{21} = \sqrt{2}/2, \\ e^p_{12} &= e^p_{21} = \frac{\sqrt{2}}{2}e^p(t), \qquad \gamma^p = 2e^p_{12}. \end{aligned} \tag{2.13}$$

Here γ^p denotes the technical measure of the angle of plastic shear. Since the only non-zero components of stress deviator are S_{11}, $S_{22} = S_{11}$, S_{33} and

$$s_{12} = s_{21} \equiv \tau,$$

where τ is the shear stress, then

$$\begin{aligned} \sqrt{\frac{3}{2}}\,Y &= \sqrt{3}\,|(\tau-\tau^R)|/2, \\ \sqrt{\frac{3}{2}}\,\pi &= \sqrt{3}\,(\tau+\tau^R)/2. \end{aligned} \tag{2.14}$$

In the case (b) the non-zero components of m_{ij} and e^p_{ij} are

$$\begin{aligned} m_{11} &= \sqrt{\frac{2}{3}}, \qquad m_{22} = m_{33} = -\frac{1}{2}\sqrt{\frac{2}{3}}, \\ e^p_{11} &= \sqrt{\frac{2}{3}}\,e^p(t), \qquad e^p_{22} = e^p_{33} = -\frac{1}{2}\sqrt{\frac{2}{3}}\,e^p(t), \qquad e^p_{11} = \varepsilon^p, \end{aligned} \tag{2.15}$$

where ε^p denotes the axial plastic strain at simple tension. Denoting by σ the axial stress the non-zero components of S become

$$S_{11} = 2\sigma/3, \qquad S_{22} = S_{33} = \sigma/3$$

and from (2.11) one obtains

$$\sqrt{\frac{3}{2}}\, Y = |(\sigma - \sigma^R)|/2,$$
$$\sqrt{\frac{3}{2}}\, \pi = (\sigma + \sigma^R)/2. \tag{2.16}$$

Note, finally, that elimination of $e^p(t)$ from (2.15) and (2.13) gives the known relationship between γ^p and ε^p

$$\gamma^p = \sqrt{3}\, \varepsilon^p$$

and that the frequently used effective plastic strain $\varepsilon_e^p = (2e_{ij}^p e_{ij}^p/3)^{1/2}$ in the case of a simple loading program (2.5) can be expressed in terms of $e^p(t)$ as folows:

$$\varepsilon_e^p = |e^p| \sqrt{\frac{2}{3}}.$$

Thus, $\varepsilon_e^p = |\varepsilon^p|$ at simple tension and $\varepsilon_e^p = |\gamma^p|/\sqrt{3}$ at simple plastic shear.

3. Experimental investigation of Y_1 and π_1 changes during cyclic loading

The experimental programs were performed at room temperature on thin tubes (outer diameter 24 mm, wall thickness 2 mm, gauge length 38 mm) made of 21CrMoV57 steel. Tension-compression and torsion in opposite directions of cyclic programs were made using the Schenck tension-compression-torsion machine connected "on line" with the HP 1000 computer (Fig. 2 machine and computer sponsored by Stiftung Volkswagenwerk). Force and moment acting on the specimen, elongation and torsion of the

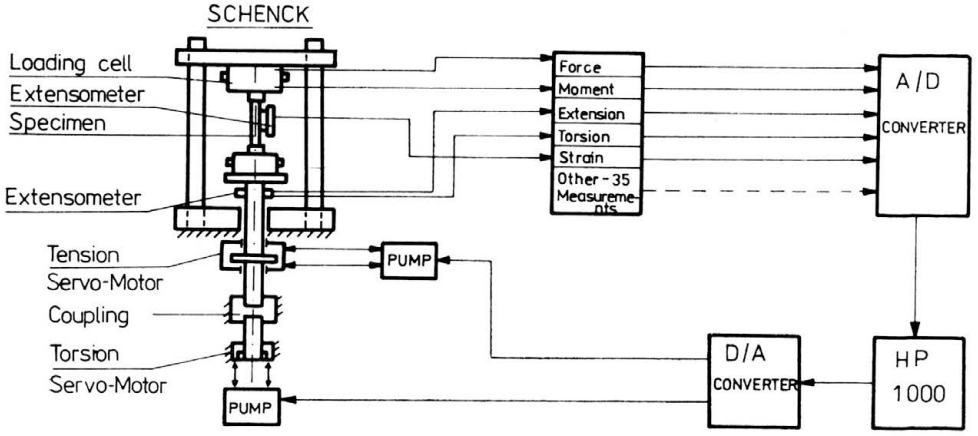

FIG. 2. The schematic diagram showing the testing machine and the computer inter-facing.

specimen, and other possible 35 measurements were read by a computer, then elaborated and the results obtained were used for the continuous machine control. The shortest time of information path: machine-computer-machine of the program used was 0.01 s.

All experimental programs were controlled by a computer programmed in FORTRAN computer language. In this case it was a symmetric cyclic program for a fixed plastic strain amplitude with a set of unloadings (loading in the opposite direction in order to determine the opposite point of the yield surface). The program was performed at a constant effective strain rate $\dot{\varepsilon}_e^p = 3.4 \cdot 10^{-4}$/s, and the actual stresses versus the logarithmic plastic strain coordinates were calculated and plotted ($\varepsilon = \ln(l/l_0)$, $\sigma = P/F_a$, where l_0 — gauge length, F_a — current specimen cross-section, P — force). Yielding was determined by the offset definition of = 0.0005, what will be discussed later (Experiment 1).

Two similar programmes were performed consisting of monotonic and cyclic loading by two kinds of stress states realised during the tension-compression tests and the reversed torsion tests of thin tubes. Details of the second program are shown below:

Symmetric cyclic torsion program

a) monotonic torsion, monotonic torsion with unloadings (Experiment 1);

b) symmetric cyclic torsion program for different plastic strain amplitudes:

I

cyclic loading for strain amplitude $\gamma^p/\sqrt{3} = \pm 0.5\%$,
cyclic loading for strain amplitude $\gamma^p/\sqrt{3} = \pm 1.5\%$,
monotonic torsion with unloadings;

II

cyclic loading for strain amplitude $\gamma^p/\sqrt{3} = \pm 1.5\%$,
cyclic loading for strain amplitude $\gamma^p/\sqrt{3} = \pm 0.5\%$,
monotonic torsion with unloadings;

III

cyclic loading with gradually increasing plastic strain amplitudes: $\gamma^p/\sqrt{3} = \pm 0.5\%$, $\pm 0.8\%$, $\pm 2.0\%$, $\pm 2.5\%$, $\pm 3\%$ (every strain amplitude change took place after reaching a stabilized loop for the former amplitude value);

IV

cyclic loading with gradually decreasing plastic strain amplitudes: $\gamma^p/\sqrt{3} = \pm 3\%$, $\pm 2\%$, $\pm 1\%$, $\pm 0.5\%$;

V

plastic pre-deformation $\gamma^p/\sqrt{3} = 2.2\%$,
cyclic loading for strain amplitude $\gamma^p/\sqrt{3} = \pm 0.5\%$,
monotonic torsion with unloadings;

VI

plastic pre-deformation $\gamma^p/\sqrt{3} = 9.2\%$,
cyclic loading for strain amplitude $\gamma^p/\sqrt{3} = \pm 1.5\%$,
cyclic loading for strain amplitude $\gamma^p/\sqrt{3} = \pm 0.5\%$,
monotonic torsion with unloadings;

Material behaviour was investigated for different cyclic loading histories, both at the steady state and during the transition periods. Here we shall present only the results

obtained for cyclic torsion. They are very similar to those obtained in the tension-compression tests in the sense, that curves

$$\sqrt{\frac{3}{2}}\,Y \text{ versus } \varepsilon^p \quad \text{and} \quad \sqrt{\frac{3}{2}}\,\pi \quad \text{versus } \varepsilon^p$$

for a cyclic tension-compression program are qualitatively similar to curves

$$\sqrt{\frac{3}{2}}\,Y \text{ versus } \gamma^p/\sqrt{3} \quad \text{and} \quad \sqrt{\frac{3}{2}}\,\pi \quad \text{versus } \gamma^p/\sqrt{3}$$

obtained in the cyclic torsion program.

Experiment 1. Monotonic torsion with unloadings (Fig. 3)

The specimen was loaded by torsion at the constant effective strain rate $\dot{\varepsilon}_e^p = 3.4-10^{-4}$/s. After every effective plastic strain increment $\Delta\varepsilon_e^p = 0.008$, the torque

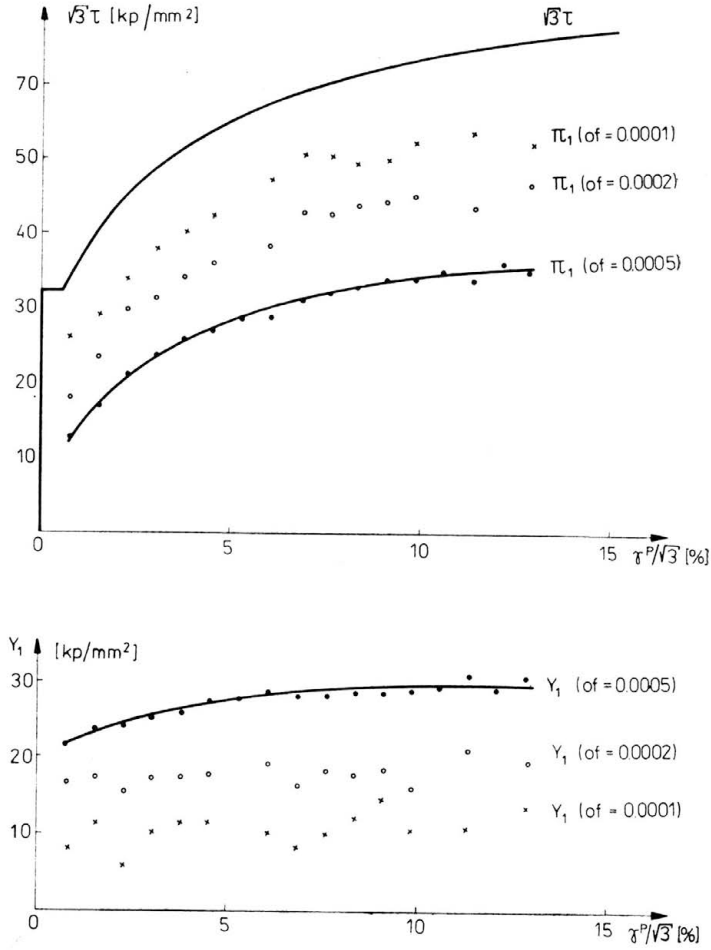

FIG. 3. π_1 and Y_1 loading curves for monotonic torsion and different yield definitions.

direction was reversed and a yield point for the new strain direction was determined, the yield "offset definition" of = 0.0005 being assumed. Once this point was reached, the former torque direction was restored. Having found such two points on the yield surface, it was possible to define the Y and π values (see Sect. 2). This type of "successive unloadings procedure" was used to define the yield surface position for different loading histories what is shown in Fig. 4 (without elastic strains). After the effective plastic strain

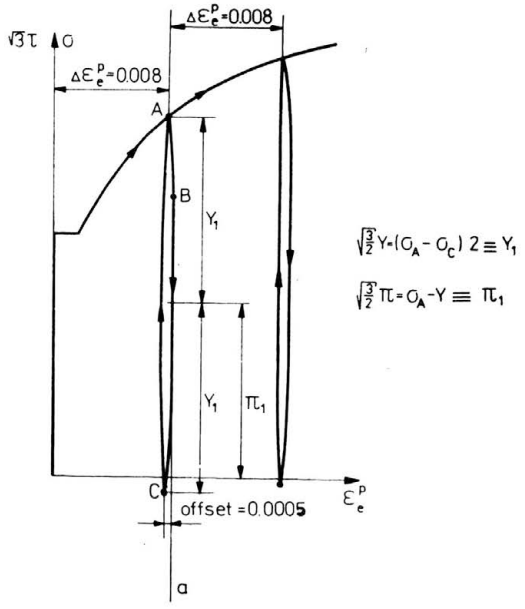

FIG. 4. Application of unloading technique for monotonic torsion.

increment $\Delta\varepsilon_e^p = 0.008$ (point A), the torque changes its direction to opposite and the slope of the unloading curve is measured. At point B (due to the rheological effects) it is equal to the Young modulus for this material and straight line a of the same slope is determined. The distance between the successive points at the unloading curve (or loading in "opposite" direction) and this line is then calculated. When it is equal to the "offset definition" the yield point is found and the torque changes its directions to the initial one.

The monotonic stress-plastic strain curve is shown in Fig. 3. Using the unloading technique at every $\Delta\varepsilon^p = 0.008$, it was possible to establish the loading path for both π_1 and Y_1, where π_1 and Y_1 are related to π and Y (Sect. 2) by the formulae

$$\pi_1 = \sqrt{3/2}\,\pi, \qquad Y_1 = Y\sqrt{3/2}.$$

They characterize the position of the centre of a yield surface and its radius, respectively.

It may be noticed that already at $\gamma^p/\sqrt{3} \approx 0.1$, the value of Y_1 reaches its maximal constant value and further hardening is caused merely by increasing π_1. In Fig. 3 the π_1 and Y_1 paths are shown for the "offset definition" of = 0.0001 ($\times$) and of = 0.0002 ($\circ$). During the experimental program controlled by of = 0.0005, the yield points corresponding to the other definitions mentioned above were also measured. Similar character

of the π_1 and Y_1 loading paths, independent of the "offset definition", is observed. Scatter of expeirmental data for of = 0.0001 shows that the unloading technique described above is not suitable for "small" yield definitions.

Experiment 2. Cyclic torsion with plastic strain amplitude $\gamma^p/\sqrt{3} = \pm 0.03$

In Fig. 5 is shown a typical stress-strain curve (without elastic strains) for a virgin material under cyclic loading with constant strain amplitude. Solid line shows the first three half-cycles, and the dashed one — the stabilized loop in the 17th and 18th half

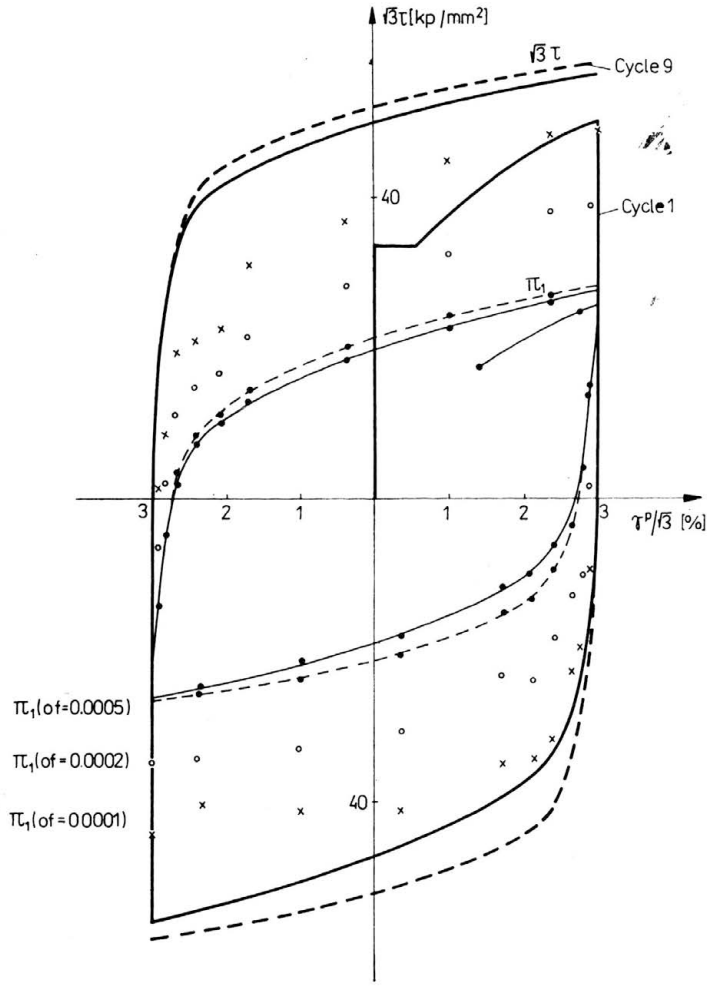

FIG. 5. Stress-strain curve and π_1 curve for cyclic torsion with constant plastic strain amplitude $\gamma^p/\sqrt{3} = \pm 0.03$.

cycles. The characteristic feature of the behaviour is that the main cyclic hardening occurs during the first three half-cycles. As before, using of = 0.0005 and the offset "unloading technique", it was possible to determine the variation of π_1 from the beginning up to the

stabilized loop. It was observed that cycles with unloadings lead to a slight material weakening. Consequently, every cycle with unloadings was followed by 3 cycles without unloadings, and so on up to the steady state. This solid line shows the π_1 curve during the first three half-cycles, and the dashed one represents the stabilized loop in half-cycles No 17 and 18. Similarly as in the case of the stress-strain curve, the general shape of the π_1-path changes abruptly during the first three half-cycles, and then remains almost constant up to the steady state. It is possible to distinguish two stages at this curve:

immediately after changing of the load direction, when small plastic strain changes are accompanied by considerable stress variation;

when considerably large strain changes are accompanied by small stress changes, and the transition period between these two stages. They can be compared with the elastic and plastic ranges of the global stress-total strain curve. Similar qualitative results, with different π_1 to Y_1 ratios were obtained for other offset definitions: of = 0.0001 (×) and of = 0.0002 (○). In Fig. 5 π_1-paths for these definitions are shown only for stabilized loops.

No π_1 hysteresis loop decay is observed, and the shape of the π_1-path for the steady state is similar to the stress-strain curve (in the steady state cycles Y_1 = const).

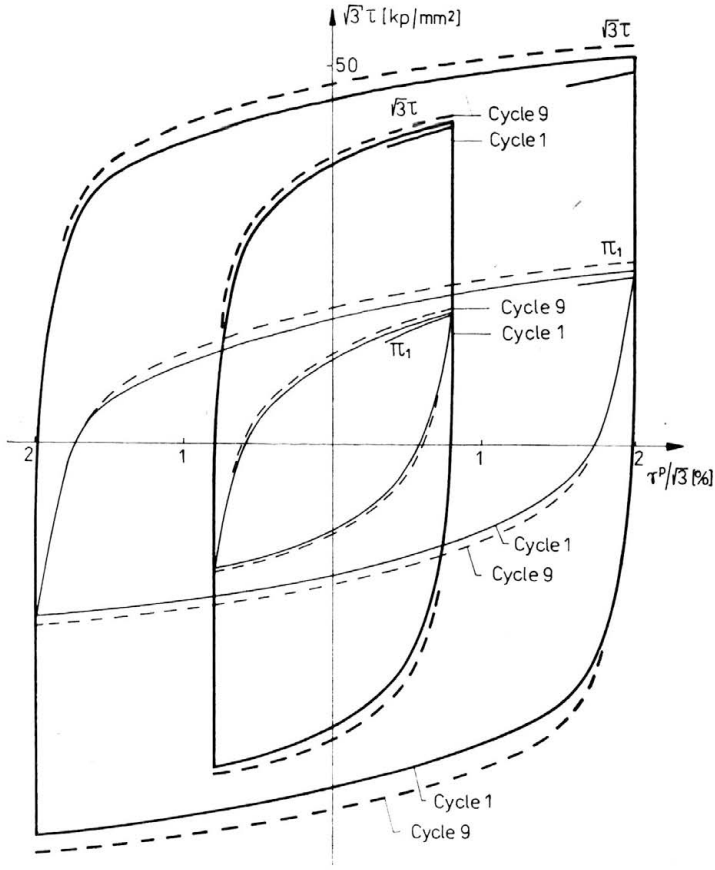

FIG. 6. Stress-strain and π_1-curves for two increasing plastic strain amplitudes.

Experiment 3. Cyclic torsion with gradually increasing plastic strain amplitudes $\gamma^p/\sqrt{3} = \pm 00.5,\ \pm 0.008,\ \pm 0.02,\ \pm 0.025,\ \pm 0.03$

The specimen was cyclically loaded with gradually increasing plastic strain amplitudes $\gamma^p/\sqrt{3} = \pm 0.005 \div \pm 0.03$. Every strain amplitude change took place after reaching the steady state cycle for the former amplitude value. In Fig. 6 are shown the stress-plastic strain curves and the π_1-curves for plastic strain amplitude $\gamma^p/\sqrt{3} = \pm 0.008$ and $\gamma^p/\sqrt{3} = \pm 0.02$. Solid line denotes the first cycle, and the dashed one — the stabilized loop. It is seen that, even though the steady state for smaller amplitude is reached, a further cyclic hardening for a greater amplitude $(\gamma^p/\sqrt{3} = \pm 0.02)$ takes place, what is visible on both the stress-plastic strain and π_1 curves.

In Fig. 7 is shown the comparison between the monotonic and cyclic skeleton curves for stress values, as well as for the values of π_1 and Y_1. In the case of cyclic curves $|\sqrt{3}\tau_{xy}|\max$, $|\pi_1|\max$ and $|Y_1|\max$ are presented for stabilized loops and different plastic

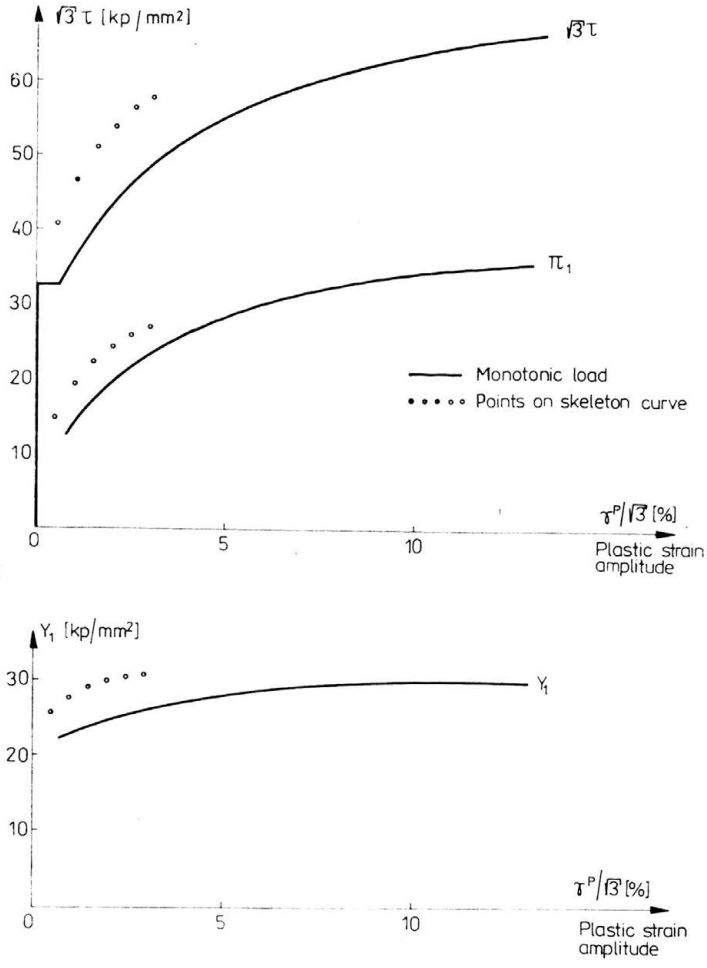

FIG. 7. Comparison between monotonic and skeleton curves for stress, π_1 and Y_1-values.

strain amplitudes. It is seen that the shapes of monotonic and skeleton curves, for both π_1 and Y_1, are similar. Cyclic curves are shifted in the direction of higher stress values. It may also be supposed that Y_1 cyclic curve also reaches its constant value for a certain strain amplitude. Unfortunately, due to technical limitations, this assumption could not be proved experimentally.

Experiment 4. Cyclic torsion with gradually decreasing plastic strain amplitudes $\gamma^p/\sqrt{3} = \pm 0.03, \pm 0.02, \pm 0.01, \pm 0.005$.

The specimen was cyclically loaded by gradually decreasing plastic strain amplitudes $\gamma^p/\sqrt{3} = \pm 0.03 \div \pm 0.005$. As before, at each stage of loading stable loops were reached. In Fig. 8 are shown the stress-strain curves and the π_1 curves for plastic strain amplitudes $\gamma^p/\sqrt{3} = \pm 0.02$ and $\gamma^p/\sqrt{3} = \pm 0.01$. Solid lines show the values during the first cycle, and dashed lines — for stabilized loops. After reaching steady state for a higher amplitude $(\gamma^p/\sqrt{3} = \pm 0.02)$ further cyclic softening for smaller amplitude $(\gamma^p/\sqrt{3} = \pm 0.01)$ is observed at both the stress-strain and π_1-curves.

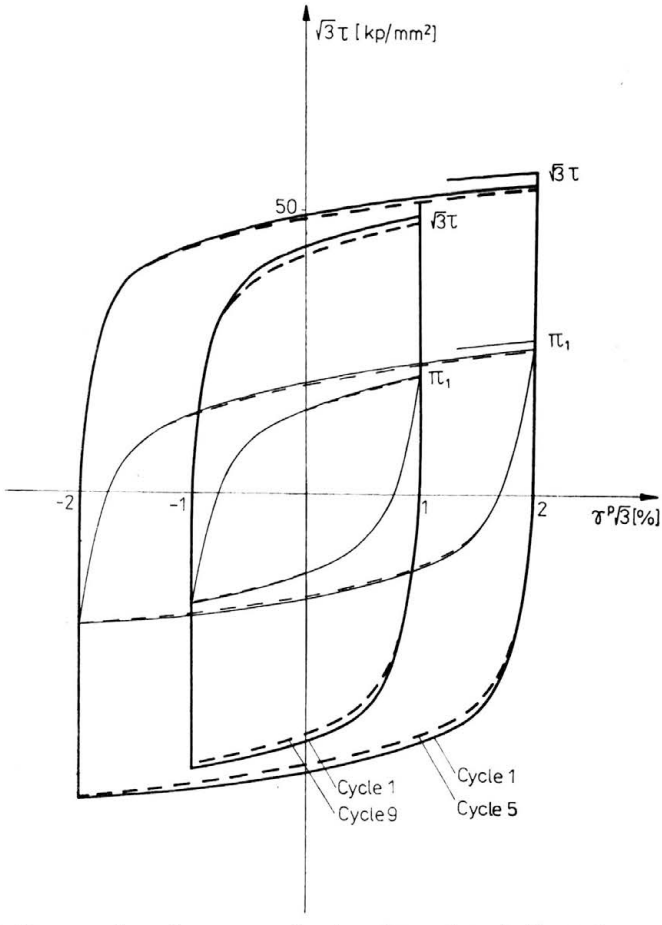

FIG. 8. Stress-strain and π_1 curves for two decreasing plastic strain amplitudes.

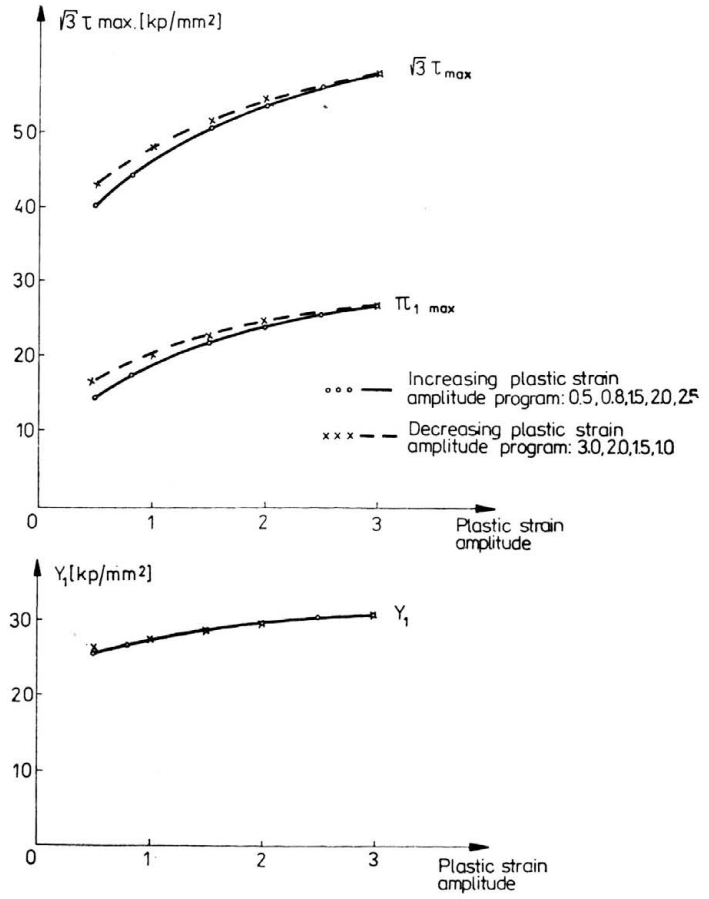

FIG. 9. Comparison between skeleton curves for stress, π_1 and Y_1 values in the case of increasing and decreasing plastic strain amplitudes.

In Fig. 9 the skeleton curves for stresses, π_1 and Y_1 values in the case of increasing plastic strain amplitudes (solid line — Experiment 3) are compared with those for decreasing strain amplitudes (dashed line — Experiment 4). It can be seen that the π_1 and Y_1 values for cyclic amplitude $\gamma^p/\sqrt{3} = \pm 0.03$ for a virgin material (first amplitude in the program with decreasing amplitude values) and for a material with the history described in the Experiment 3 are the same. Discrepancy between the solid and dashed lines indicates the influence of the cyclic loading history at higher amplitudes on the material behaviour under cyclic loading at smaller amplitudes. However, no such influence on the values of Y_1 was observed.

Experiment 5. Influence of cyclic history on the material behaviour under monotoning loading

Virgin specimen was cyclically loaded with plastic strain amplitudes $\gamma^p/\sqrt{3} = \pm 0.015$ and then $\gamma^p/\sqrt{3} = \pm 0.005$ up to the stabilized loop, and afterwards monotonically twisted until rupture, at a constant strain rate $\dot{\varepsilon}_e^p = 3.4 \cdot 10^{-4}/\text{s}$. Using the unloading technique

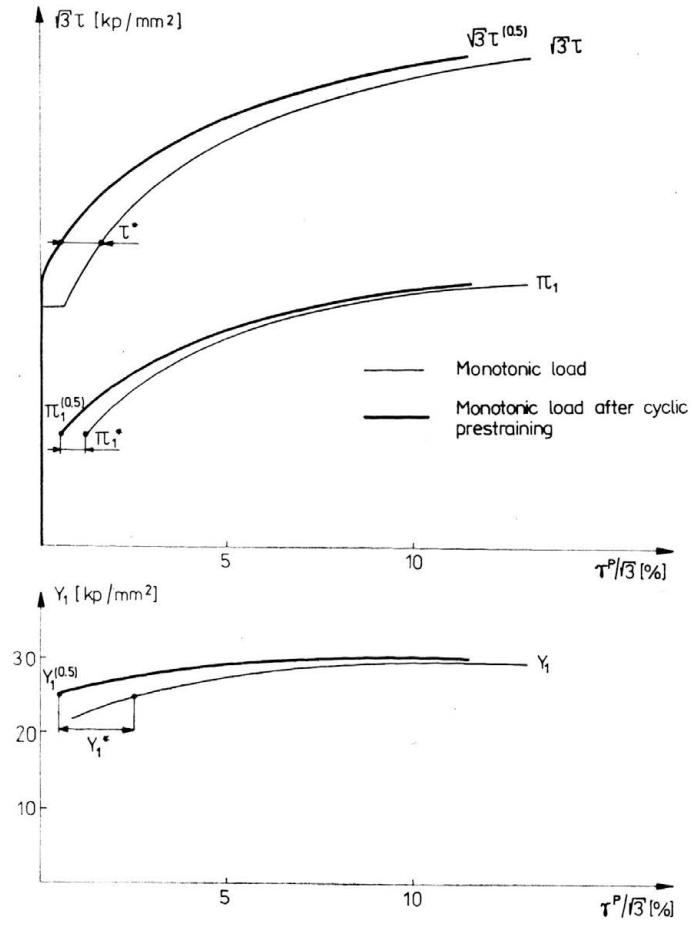

FIG. 10. Comparison between stress-strain, π_1 and Y_1 monotonic torsion curves with corresponding curves after cyclic pre-straining with plastic strain amplitude $\gamma^p/\sqrt{3} = 0.005$.

it was possible to determine the monotonic π_1 and Y_1 curves. In Fig. 10 they are compared with the corresponding curves obtained for a virgin material. Due to cyclic pre-loading, material hardening in stress, π_1 and Y_1 values is observed. Their maximal values at stabilized loops for the strain amplitude $\gamma^p/\sqrt{3} = 0.005$ are denoted by $|\sqrt{3}\tau_{xy}|^{0.5}$, $|\pi_1|^{0.5}$ and $Y_1^{0.5}$. Now, shifting the monotonic curves obtained for monotonic torsion after pre-cycling program to the points corresponding to $|\sqrt{3}\tau_{xy}|^{0.5}$, $|\pi_1|^{0.5}$ and $Y_1^{0.5}$ on such curves obtained for virgin material (τ^*, π_1^*, Y_1^*), it can be seen that these curves coincide.

Experiment 6. Infiuence of plastic prestrain on the subsequent cyclic behaviour

The specimen was plastically prestrained up to $\gamma^p/\sqrt{3} = 0.092$ and then cyclically loaded with plastic strain amplitude $\gamma^p/\sqrt{3} = \pm 0.015$. The stress-strain and π_1 cyclic curves are shown in Fig. 11. After hardening caused by plastic prestrain, cyclic relaxation

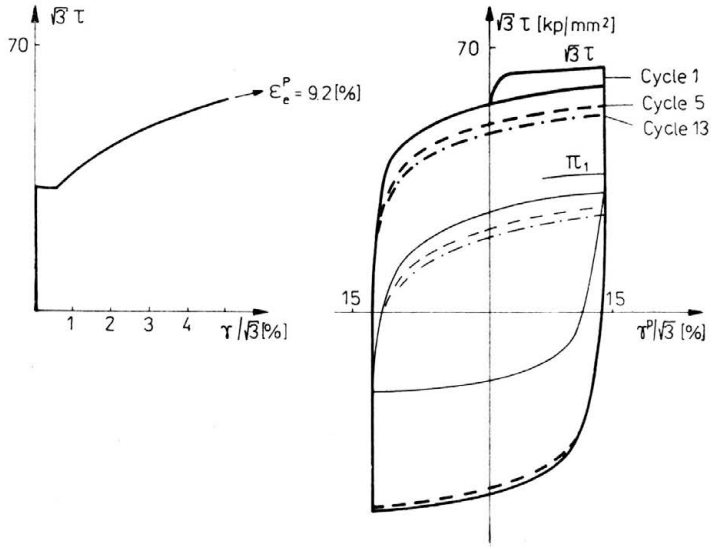

FIG. 11. Stress-strain and π_1 cyclic curves for plastic strain amplitude $\gamma^p/\sqrt{3} = \pm 0.015$ after plastic prestrain $\gamma^p/\sqrt{3} = 0.092$.

of stresses and π_1 in the prestrain direction is observed. However, in the opposite prestrain direction the shapes of the stress-strain and the π_1 curves remained almost unchanged from the very beginning.

4. Concluding remarks

Summing up the results obtained, the following conclusions may be drawn:

1) When the succesive actual yield surfaces are approximated by ellipsoids, the values of π_1 and Y_1 measured here may directly be identified with the hardening parameters. The presented experimental results illustrate the evolution of these parameters for two cyclic and monotonic simple paths in the plastic strain space. They supply new information which can stimulate new theoretical ideas.

2) General shape of the π_1 path during cyclic loading is established during the first full cycle, and then it changes but slightly to reach a stable loop. Shape of this loop is similar to the stress loop (Y_1 = const), and no decay of the π_1 hysteresis loop is observed.

3) Shapes of the monotonic and skeleton curves for stresses, π_1 and Y_1, are similar, the cyclic ones being shifted in the direction of higher stresses.

4) No effect of the strain history on the value of Y_1 at steady state is observed. The value of Y_1 under cyclic loading at a steady state depends merely on the strain amplitude.

5) Slight quantitative influence of the cyclic history on the subsequent cyclic behaviour is observed in $|\pi_1|_{\max}$ and $|\sqrt{3}\tau_{xy}|_{\max}$ values at fixed plastic strain amplitudes.

6) Cyclic loading after plastic prestrain leads to the relaxation of stresses and π_1 in co-prestrain direction; in the counter-prestrain direction the shapes of the stress–strain and π_1 curves remain almost constant from the beginning of the cyclic program.

Acknowledgement

This work was carried out while two of us (B. R. and W. T) held the Alexander von Humboldt Fellowships in Germany. The generosity of the Foundation, help of VW Stiftung in performing the experimental program and hospitality of the Institute of Mechanics I at Bochum University are gratefully acknowledged.

References

1. Z. MRÓZ, *On generalized kinematic hardening rule with memory of maximal prestress*, J. Mech. Appl., 5, 242–260, 1981.
2. J. CHABOCHE, *Viscoplastic constitutive equations for the description of cyclic and anisotropic behaviour of metals*, Bull. Acad. Polon. Sci., **25**, 1, 39–47, 1977.
3. T. LEHMANN, *General frame for the definition of constitutive laws for large non-isothermic elastic-plastic and elastic-visco-plastic deformations*, The Constitutive Law in Thermoplasticity, CISM, 1984.
4. B. RANIECKI, *Thermodynamic aspects of cyclic and monotone plasticity*, The Constitutive Law in Thermoplasticity, CISM, 1984.
5. E. SHIRATORI, K. IKEGAMI, K. KANEKO, *Subsequent yield surface determined in consideration of the Bauschinger effect*, Foundations of Plasticity, ed. by A. SAWCZUK, Nordhoff, 477–490, 1973.
6. A. PHILIPS, J. TANG, M. RICCIUTI, *Some new observations on yield surfaces*, Acta Mech., **20**, 23–39, 1974.
7. W. SZCZEPIŃSKI and J. MIASTKOWSKI, *An experimental study of the effect of the prestraining history in the yield surfaces of an aluminium alloy*, J. Mech. Phys. Solids, **16**, 153–162, 1968.
8. K. IKEGAMI, *Experimental plasticity on the anisotropy of metals*, Proceedings of the Euromech Colloquium, 115, 1979, ed. J. BOEHLER, 1982.
9. R. MARIANOVIC and W. SZCZEPIŃSKI, *On the effect of biaxial cyclic loading on the yield surface of* M-63 *brass*, Acta Mech., **23**, 65–74, 1975.
10. J. MIASTKOWSKI, *On the effect of the two-dimensional cyclic loadings on the yield surface of an aluminium alloy*, Bull. Acad. Polon. Sci., **26**, 5, 221–229, 1978.
11. M. ŚLIWOWSKI, *Behaviour of stress-strain diagrams for cyclic loadings*, Bull. Acad. Polon. Sci., **27**, 2, 115–123, 1979.

BOCHUM UNIVERSITY, FRG

and

POLISH ACADEMY OF SCIENCES
INSTITUTE OF FUNDAMENTAL TECHNOLOGICAL RESEARCH.

Received April 19, 1985.